

A E Harris, P M Render, O M Pozniak, M E Wood  
Aircraft Research Association Ltd,  
Manton Lane, Bedford MK41 7PF, UK

ABSTRACT

In recent years the ARA has been engaged in a substantial series of contra-rotating propeller (CRP) wind-tunnel based research programmes. All programmes have been undertaken within a UK club arrangement involving British Aerospace, Rolls-Royce, Dowty Aerospace and the ARA, with Department of Trade and Industry and Royal Aerospace Establishment support. Advances in experimental techniques have led to the capability to perform research in the following areas:

- Small scale isolated and installed CRP testing using compressed air driven turbine motors to study rotors of typically 0.4 m diameter;
- Large scale isolated testing using electric motor driven CRP models of typically 0.8 m diameter;
- CRP performance studies using rotating shaft mounted balances at large and small scale;
- Noise field studies using an acoustically lined wind tunnel in parallel with CRP performance measurements;
- Flow field surveys supported by 'club' laser and conventional measurements.

The paper sets out to review all of the above techniques within the broad context of experimental research on advanced rotor designs.

NOTATION

BPF	Blade passing frequency
$C_D, C_{DRAG}$	Drag coefficient
$C_{DISCH}$	Nozzle discharge coefficient
$C_{LIFT}$	Lift coefficient
$C_P, C_{POWER}$	Power coefficient = power/ $\rho \cdot N^3 D^5$
$C_T, C_{THRUST}$	Propeller thrust coefficient = thrust/ $\rho N^2 D^4$ also nozzle thrust coefficient
CQ	Torque coefficient = torque/ $\rho N^2 D^5$
D	Propeller diameter
f	Frequency
J	Advance ratio = V/ND
$M_\infty$	Free stream Mach number
N	Propeller rotational speed, rotations per second
NPR	Nozzle pressure ratio
$P_\infty$	Free stream static pressure
V	Free stream velocity
$\alpha$	Incidence
$\beta$	Blade angle
$\delta, \Delta$	Increment
$\Delta D_S$	Increment in body drag due to slipstream
$\eta$	Propeller efficiency
$\theta$	Polar angle
$\rho$	Free stream density

Subscripts

F	Pertaining to front rotor
O	Overall (front + rear)
R	Pertaining to rear rotor
MAX	Maximum
MIN	Minimum

ABBREVIATIONS

Able	Able Corporation, Anaheim, Ca, USA
AC	Alternating current
ADC	Analog to digital converter
ARA	Aircraft Research Association Ltd
BAe	British Aerospace (Commercial Aircraft) Ltd, Hatfield, England
CF	Centrifugal force
CFD	Computational fluid dynamics
CRP	Contra-rotating propellers
DA	Dowty Aerospace Gloucester Ltd
DTI	Department of Trade & Industry
HP	High pressure (air)
Hz	Hertz
LTA	Laser transit anemometry
MOD	Ministry of Defence
MST	Mach Simulation Tank
MTR	Microphone Traverse Rig
NC	Numerical control
RAE	Royal Aerospace Establishment
RR	Rolls-Royce plc
SPARV	Source Patch & Ring Vortex
SRP	Single rotation propeller
TD	Tech Development Inc, Dayton, Ohio, USA
TWT	ARA transonic wind tunnel

1 INTRODUCTION

The objective of this paper is to recount recent ARA experience related to contra-rotating propeller (CRP) research. Whilst ARA involvement in the CRP design process will be reported elsewhere, the aim here is to illustrate the diverse nature of the large and small scale CRP experimental studies in which ARA has participated.

Experimental work on advanced propellers began at ARA in the mid 1980s, with the aim of establishing a capability to make accurate aerodynamic, acoustic and performance measurements on open rotors in the ARA transonic wind tunnel<sup>1</sup>. The sequence of experimental programmes to date is shown in Figure 1. The dominant feature of all of the programmes outlined in Figure 1 is that they are jointly funded 'club' activities; these club activities have systematically involved the appropriate specialists drawn from industry including particularly Rolls-Royce, British Aerospace and Dowty Aerospace as well as significant work placed with smaller companies; all work has received substantial support from the UK Department of Trade and Industry and has benefited from active involvement of RAE specialists.

As shown in Figure 1 the emphasis of the programme has moved in recent years from single rotating propellers (SRP) to cover the more challenging CRP research needs. In total these needs are:

- Overall and individual rotor performance (thrust, torque, power, efficiency) at on- and off-design conditions;

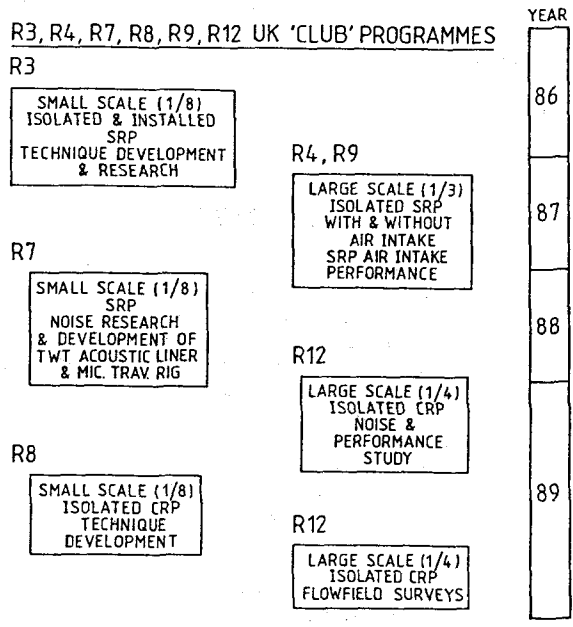


FIG 1 ARA INVOLVEMENTS IN UK OPEN ROTOR RESEARCH CLUB PROGRAMMES

- b) CRP near field and far field noise spectra at on- and off-design conditions;
- c) Isolated CRP performance/noise data base for evaluation of CFD predictions;
- d) Flow field and blade/nacelle pressure data to permit evaluation of local performance contributions and to enable the empirical elements in prediction methods to be improved or replaced;
- e) Blade strain gauge and blade 'live' twist data to supplement rotor finite element structural analyses and to refine aerodynamic 'live' blade CFD modelling;
- f) Isolated rotor slipstream surveys as an aid to installation and air intake design activities;
- g) Techniques of proven capability for CRP project developments;
- h) Installed CRP performance data.

All of the above objectives have played a part in the formulation of the research studies discussed here.

In the following sections salient features of the more recent CRP activities are discussed. It is noted that many of the techniques employed in the SRP and CRP research studies derive, in part, from the established powered testing techniques in use at ARA in support of isolated and installed conventional turbofans<sup>2</sup>.

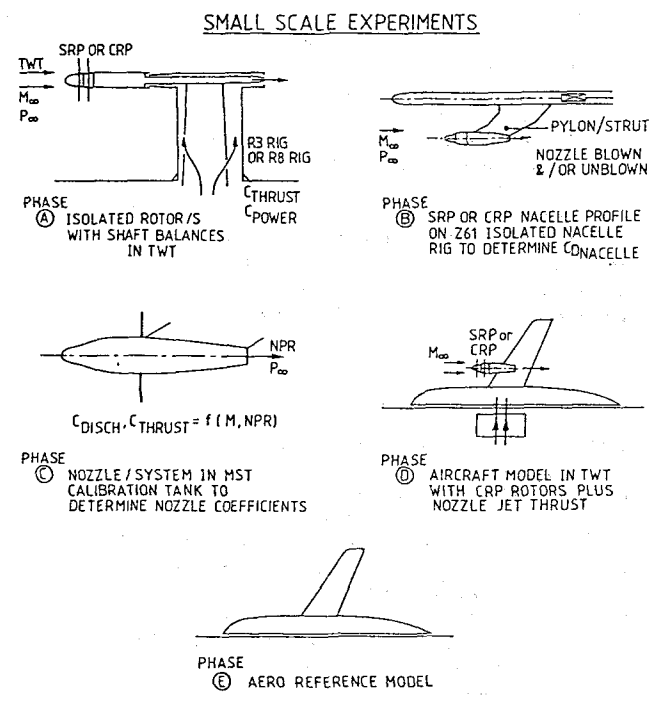
**2 SRP AND CRP INSTALLATION DEVELOPMENT STUDIES**

Figure 2 shows an overview of a large and small scale model development testing methodology leading to a well engineered installation for an SRP or CRP powered aircraft. The five test phases A to E are used in a combined manner to assess overall rotor and installation aerodynamic performance in line with an appropriate thrust/drag accounting framework<sup>3</sup>. The large scale rig of phase F is used to extend understanding of isolated rotor performance as well as to study (or further study)

rotor noise and to examine air intake/rotor interaction performance. Further discussion of large scale studies is deferred to section 4 below.

The five small scale test phases illustrated in Figure 2 yield an assessment of installed SRP or CRP interference drag.

This capability to evaluate those elements of overall drag which may be classified as 'interference' is a vital factor in the development of high speed rotor powered aircraft. It is clear that Figure 2 presents an over-simplified version of the practical accounting steps involved. Factors not listed in the scheme include the substantial pre-model design/prediction stages of both rotor performance and installation design. The assessment of overall aircraft/rotor performance is the province of airframe and propulsion specialists; recognising this, the remainder of this paper concentrates on the research facilities which provide the data base for such assessments.



**THRUST/DRAG ACCOUNTING\***

$$\text{CRP/NACELLE INTERFERENCE DRAG} = \left[ \begin{matrix} \text{A/C + CRP + NACELLE + JET} \\ \text{DRAG Phase (D)} \end{matrix} \right] - \left[ \begin{matrix} \text{JET THRUST} \\ \text{based on Cal. Phase (C)} \end{matrix} \right]$$

$$- \left[ \begin{matrix} \text{CRP THRUST} \\ \text{based on Phase (A)} \end{matrix} \right] - \left[ \begin{matrix} \text{NACELLE DRAG} \\ \text{based on Phase (B)} \end{matrix} \right]$$

$$- \left[ \begin{matrix} \text{CLEAN A/C DRAG} \\ \text{Phase (E)} \end{matrix} \right]$$

\*The above scheme oversimplifies accounting; full accounting uses various assessments of incremental terms such as  $\Delta D_s$  and embodies supplementary test phases / builds.

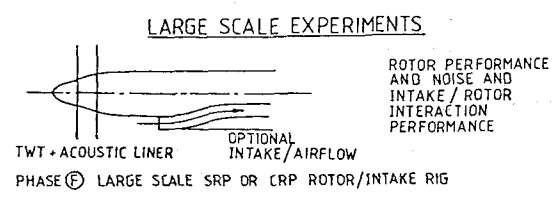


FIG 2 OVERVIEW OF SRP OR CRP INSTALLATION DEVELOPMENT PROGRAMME

### 3 SMALL SCALE CRP EXPERIENCE

#### 3.1 Special Rig for Isolated CRP Tests

In the period 1988/90 a small scale model CRP technique has been evolved to cater for isolated and installed testing in answer to the combined requirements of British Aerospace, Dowty Aerospace, the DTI and ARA.

The thrust, torque and power accounting schemes for an SRP or CRP invariably require a clear description of the contributions of the rotor, the nacelle and the nozzle elements of the powerplant installation. Figure 3 shows the main features of a high speed wind tunnel rig developed specifically for support of CRP isolated small scale studies. At the rig design stage, considerations of rig structural survival in the event of loss of a blade, or blades, led to a robust strut mounted assembly; a non-metric shield is provided to minimise concerns regarding the effects of CRP slipstream on the downstream rig elements. The rig is mounted on a well established underfloor balance; The key feature of the rig is the provision of two shaft mounted rotor force and moment balances; these balances are used for evaluation of rotor/hub thrust, torque and power (see section 3.2).

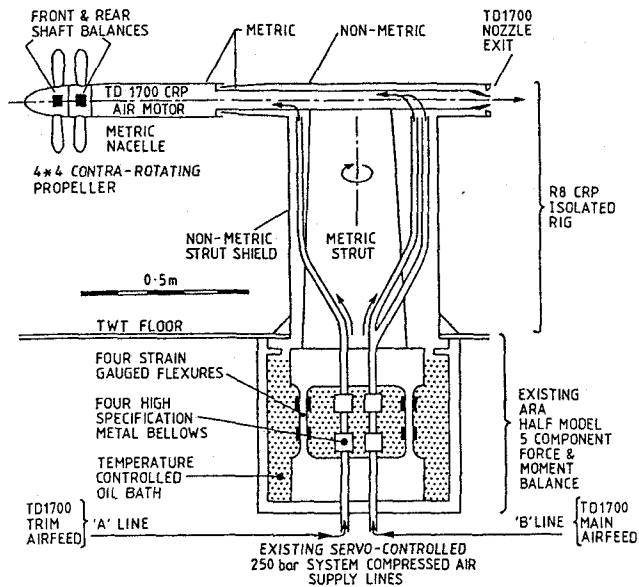


FIG 3 R8 TRANSONIC WIND TUNNEL INSTALLATION

Power for the model CRP is provided using a British Aerospace owned Tech Development TD1700 air motor and much of the rig development programme was concerned with the capability to provide precisely controlled power to the individual CRP stages. Tests in both an out-of-tunnel test house at  $M = 0$  and in the ARA 2.7 m x 2.4 m transonic wind tunnel (to  $M = 0.8$ ) have demonstrated that the individual rotors can be controlled to around  $\pm 0.1\%$  of rotor speed in spite of the rotor-to-rotor interactions.

Following normal ARA practice the rotors of the CRP small scale installations, on rig or aircraft model, are cleared using blade mounted strain gauges. The outputs of the strain gauges are used as a means of assessing rotor dynamic disturbances, critical points and flutter. In addition, the rig is equipped with accelerometers and these are used

to supplement blade strain gauges and shaft balance data to give overall blade, rotor and rig dynamic data.

It is noted here that it is necessary, as illustrated in Figure 2, to determine the thrust of the model exhaust nozzle. The use of an underfloor compressed air feeding force balance, wherein the air travels into the metric model system perpendicular to the thrust axis, permits a simple treatment of nozzle thrust based on nozzle coefficients. A set of experiments in the Mach Simulation Tank (MST) is used to determine the nozzle thrust and discharge coefficients in a quiescent exhaust environment. Use of common critical venturi meters (for turbine drive air flow measurement) in the airfeed to the MST and TWT allows the linking of nozzle airflow accounting procedures to enhance security of the derived data<sup>2</sup>.

#### 3.2 Development of Shaft Mounted Thrust/Torque Balances

Following on from the successful development of shaft mounted thrust/torque measurement strain gauged balances for SRP application, the requirements for a pair of CRP balances have been addressed. Key features of these balances were as follows:

- Transmission of balance electrical signals by slipring for the front rotor and telemetry for the rear rotor;
- Mounting of balances to shaft and rotor hubs designed to minimise stress 'signatures' at the balance flexures, and
- Thermal problems arising due to heat flow along the CRP shafts to the cold air motor turbines to be minimised by design.

The compact nature of the model led to the overall hub design scheme outlined in Figure 4. The attachments to both the shafts and to the rotors were specifically designed to produce a symmetric low-stress torque and thrust path to the balance flexures.

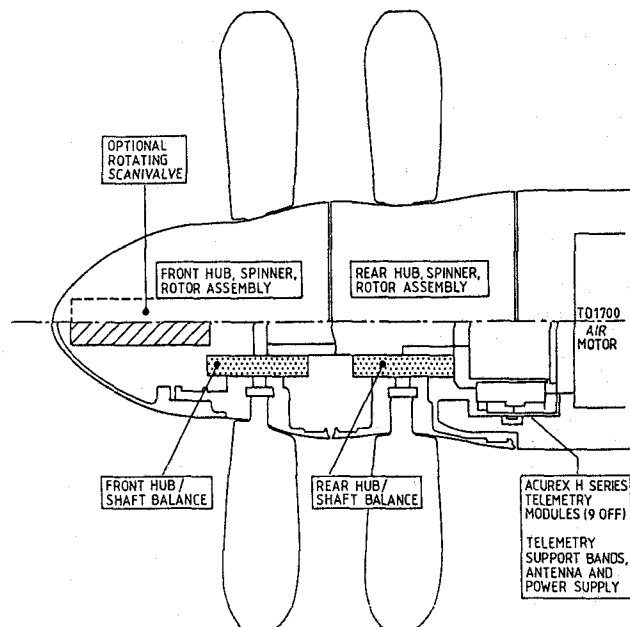


FIG 4 R8 FRONT AND REAR HUB ASSEMBLIES

The shaft strain gauged balance design, Figure 5, comprises a set of suitably disposed flexures in a basically symmetrical layout with strain gauges placed so as to provide symmetry and duplication of the key elements. A high standard of accuracy was achieved using a layout of multiple compensating gauge placements which were devised to minimise the problems noted in b) and c) above. In particular, the design aim of a balance giving  $\pm 1\%$  repeatability in a static calibration was successfully achieved.

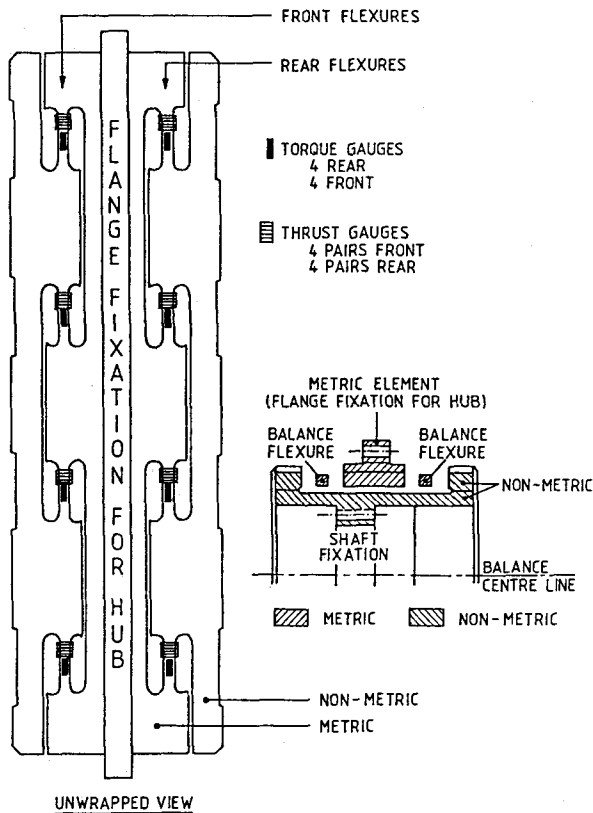


FIG 5 ARA PROPELLER BALANCE

Development of the required telemetry installation to support the above accuracy target was not without problems. The high CF loads required a specially configured housing for nine telemetry units. Considerable care was necessary to ensure that the telemetry unit installation met exacting electrical and structural requirements. Special composite retention rings were designed into the telemetry unit housing scheme and a high ( $\pm 1\%$ ) standard of signal processing resulted from the detailed electrical and structural refinements. The telemetry units were used for transmission of the strain gauged balance signals as well as signals from blade mounted strain gauges.

### 3.3 Propeller Blades and Hubs

The high stress levels arising in small scale propellers necessitate the closest attention to detail in all aspects of blade and hub design and manufacture. Blades are fabricated from selected bar stock titanium to a high tolerance on profile and twist distribution. Key features in the production of model blades are the analysis of the blade-to-shank structural region and blade sections

using finite element stress analysis methods to arrive at a geometry giving the required aerodynamic profiles yet moderate peak stress levels. The studies have invariably benefited from the wide experience of rotor 'club' partners in this process, especially in respect of the aero/structural design and in relation to blade dynamic stress assessments. In order to achieve the required blade surface finish to minimise risks of fatigue failure, blades were hand finished and polished after NC machining.

The method of attachment of rotor blades to hubs was an important feature of the hub design. In order that any selected set of blade angles could be created in the front and rear blade rows, a clamping scheme was used to hold and secure the blade shanks. The design of this feature necessarily included a shank blend region to minimise stress concentrations at the blade/hub/shank interface region as well as blade retention and setting features. In practice, it has been shown that consistent blade settings to the order of  $\pm 0.1^\circ$  have been achieved.

The availability of an infinitely variable blade angle setting/clamping scheme has enabled settings to be adjusted to correct for errors in predicting the model rotor 'live' twist which arises from the combined aerodynamic and dynamic loading of the elastic blades.

The design of the rotating components had to allow for dynamic loads. Significant cyclic stresses arise due to operation with combinations of high power and angle of attack. A relatively conservative level of cyclic stress has been allowed within the working stress envelope; maximum allowable cyclic stress levels were based on factoring of the infinite fatigue life value.

In overall terms the design and integration of blades, hubs, shaft balances, sliprings and telemetry units has represented a significant engineering challenge.

### 3.4 Software Systems for CRP Test Support

The control and surveillance of tests using compressed air driven air motors with shaft balance supported CRP hubs and rotors makes significant demands on computer software systems for test support. Figure 6 shows the overall scheme of computers and data system used to provide on-line real-time assimilation of model and air motor 'health' and performance data. In addition, the more traditional analogue and dynamic data analysis techniques are required for ensuring acceptable margins on blade stress and related rig dynamics.

The overall monitoring and control of the test falls into two categories:

- Continuous on-line rig/rotor/motor control/'health' parameter monitoring;
- Review of on-line performance data to ensure collection of suitable sets of parametric performance data.

The category a) data is provided in timescales of 0.1 to 0.2 seconds, whereas the delay time for plotted category b) data is in the region of 10 seconds.

### 3.5 Typical Test Data for Small Scale Isolated CRP

A typical isolated CRP operating matrix is illustrated in Figure 7. In general, it is unlikely that the measured CRP performance will match the predictions. Some of the reasons are:

- Unpredicted blade root and tip region performance,
- Front to rear rotor flowfield interference,
- Non-correspondence of predicted and actual front and rear rotor blade 'live' twist,
- Deviation of measured from predicted rotor efficiency variations,
- Lack of completeness of the prediction computational model,
- Scale effects due to lower test Reynolds numbers.

In the course of producing the CRP performance data it has been found that the blade setting angles required to produce a given level of thrust fall very close to the predictions and that the general form of thrust, power and efficiency variations are largely predictable. The actual levels of efficiency are, however, found to deviate slightly from the design point predictions; for conditions far away from the design point deviations are more marked.

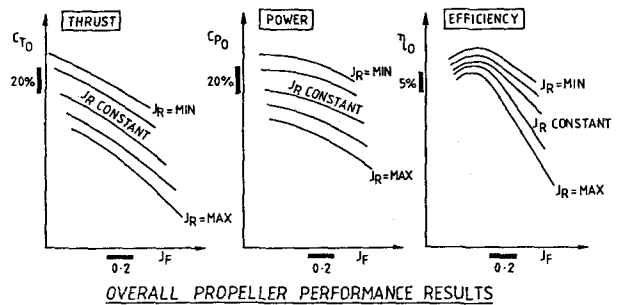
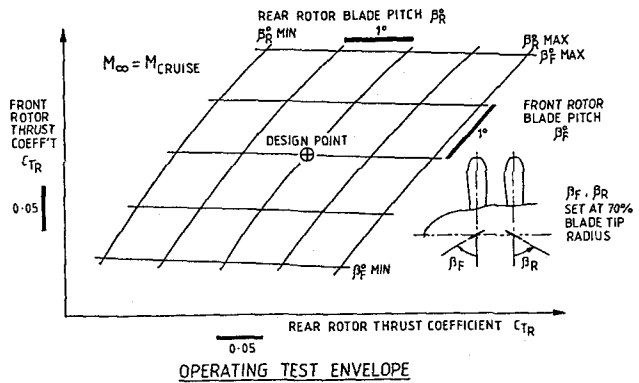


FIG 7 OPERATING MAP FOR SMALL SCALE ISOLATED CRP

## 4 LARGE SCALE CRP EXPERIENCE

### 4.1 Objectives of Large Scale CRP Programme

The most recent and most substantial of the club activities on open rotors has been the R12 research programme on contra-rotating propellers of 0.8 m diameter. The main objectives of this programme were:

- Acquisition of CRP performance data for comparison with CFD based predictions;
- Measurement of near field and far field noise;
- Evaluation of a laser based method to measure 'live' blade twist and camber;
- Slipstream measurements using rakes placed downstream of the CRP;
- Application of laser holographic flow visualisation to CRP in a high speed wind tunnel;
- Study of CRP flow fields using laser transit anemometry;
- Measurement of blade surface pressures using flush mounted pressure transducers (steady and dynamic signals);
- Use of a telemetry system for transmission of all data from rotor mounted sensors, including shaft mounted balances;

The programme covered two designs of CRP and there were two separate test series in the transonic tunnel. In the first of these noise and performance data were obtained and in the second flow field surveys were made. In the following sections the main characteristics of the rig and the results of the programme are outlined.

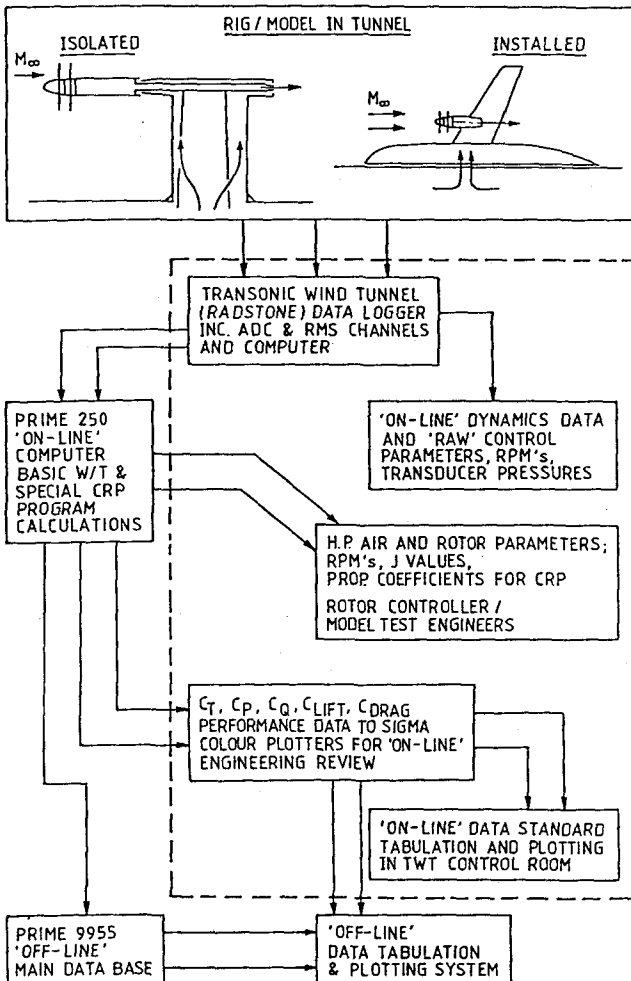


FIG 6 DATA SYSTEM FOR SMALL SCALE CRP TESTS

## 4.2 Motors and Rig

At an early stage in the overall propeller research programme, the need for a compact, high powered propeller drive for the transonic wind tunnel was recognised. The leading requirements were:

- Total power in the region 1000 to 1200 SHP (750 to 900 kW);
- Provision for SRP or CRP capability with power equally divided between shafts;
- Long power-on testing endurance for maximising tunnel productivity;
- Accurate and rapid rotational speed control (order  $\pm 0.1\%$ ) for SRP or CRP;
- Long mean-time-between-overhauls and high operational reliability;
- Low noise to minimise adverse effects on propeller noise research;
- Minimal contamination of wind tunnel circuit airflow to retain maximum tunnel productivity.

These requirements were met by a pair of AC induction motors made by Able Corporation of the USA, fed from a pair of inverters giving a variable frequency supply to 360 Hz quasi-AC. The main characteristics of the motors are:

- Power per shaft 660 SHP (490 kW) at 7000 rpm;
- Envelope size per motor 25" long (0.63 m) by 14" diameter (0.36 m);
- Weight per motor 850 lbs (385 kg);
- Integral lubrication and cooling scheme.

The motors were first used in the R4 and R9 programmes on single rotation propellers<sup>1</sup>. For the CRP programme, they were incorporated into a specially constructed Rolls-Royce rig (Rig 140).

This rig is shown installed in the transonic tunnel in Fig 8. The upper diagrams show the rig installed together with the acoustic liner for the combined performance and noise measurements of the first test series; the lower diagrams show the installation in the basic tunnel for the combined performance and flow field survey of the second series.

As shown in the lower diagram, the two Able motors were mounted in the rig in tandem. A structural sleeve was used to carry the motors ahead of a robust sting; the sting, in turn, was pivoted from a large strut which traversed vertically so that, as propeller angle of attack was varied, the CRP remained in the centre of the tunnel working section. The CRP nacelle and rotors were developed by Rolls-Royce with support in respect of rotor design and rig integrity from Dowty Aerospace and ARA. The components of the CRP assembly consist of

- the drive shaft coupling module;
- the CRP module front and rear rotor elements;
- the non-rotating nose bullet;
- an extensive rig health and performance instrumentation system.

A co-axial system of three shafts connects the rotors and bullet to the Able electric motors; the inner stationary shaft is used to prevent rotation of the bullet although bullet structural support is given by the CRP module.

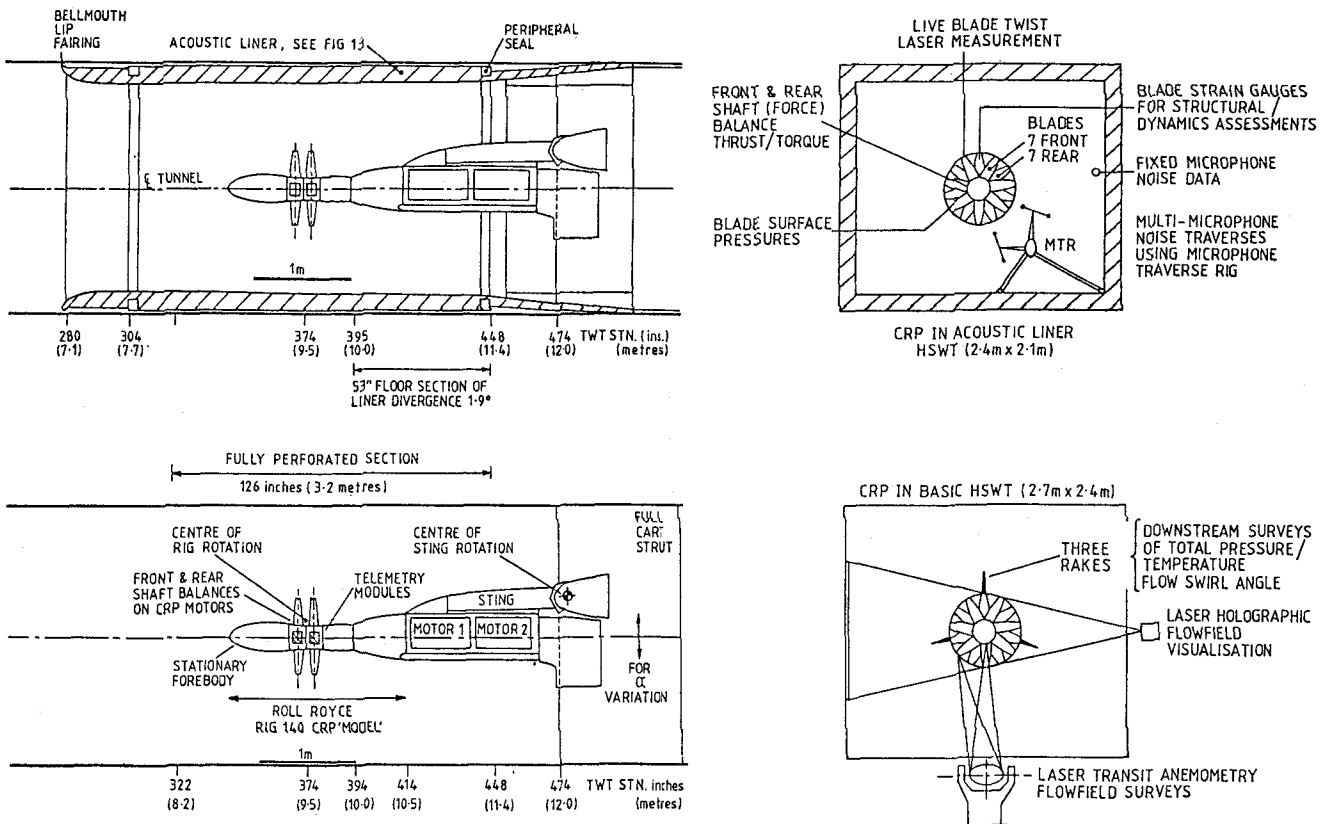


FIG 8 CRP MEASUREMENTS DURING TESTS IN ACOUSTIC-LINED & BASIC HIGH SPEED TUNNEL

### 4.3 Rig and Model Instrumentation

The primary instrumentation of the rig was a pair of shaft mounted thrust and torque balances and a substantial set of surface static pressures to enable rotor performance to be evaluated, coupled with extensive rig and rotor 'health' instrumentation including, in particular, strain gauges on the rotor blades.

In addition, a set of blade mounted (flush) pressure transducers was provided for assessment of dynamic and steady state pressure variations (Figure 9); also, a system for measurement of front and rear rotor blade 'live' twist and camber was evaluated. These measurements will contribute to a more thorough understanding of the comparisons between predicted and measured CRP performance. The 'live' twist measurements may also be used to improve the aero/structural prediction models which are necessary for realistic prediction of rotor aerodynamics.

The test programme included an assessment of the likely effects of the excrescences on the rotor blade surfaces due to the placement of pressure transducers and strain gauges (and all associated wiring); in the first test series a set of totally clean blades was included for performance and noise measurement purposes.

The acoustic measurements of the first test series were made on a set of fixed microphones and on a mobile microphone array mounted on a microphone traverse rig as shown in the upper part of Fig 8. For the flow field measurements of the second test series, a set of three downstream rakes provided surveys of slipstream total pressure, swirl angle and total temperature and, as shown in the lower part of Fig 8, laser transit anemometry and laser holography systems (see section 4.4) were deployed.

The overall data system was similar to that used for small scale CRP work, as shown in Figure 6; however, a number of additions were embodied for the large scale work. Figure 10 shows the R12 network of signals and monitoring functions.

The leading facets of rig/model health and control were as follows:

- a) Dynamic analysis of blade strain gauge, pressure transducer and accelerometer signals, on-line and using recorded sequences;
- b) Monitoring of test management computer data covering bearing temperatures, lubrication system and cooling system performance, on-line;
- c) Assessment of real-time Able motor/Cortina inverter data to ensure compliance with established operational requirements;
- d) Surveillance of conventional forces and pressures data signals using established methods;

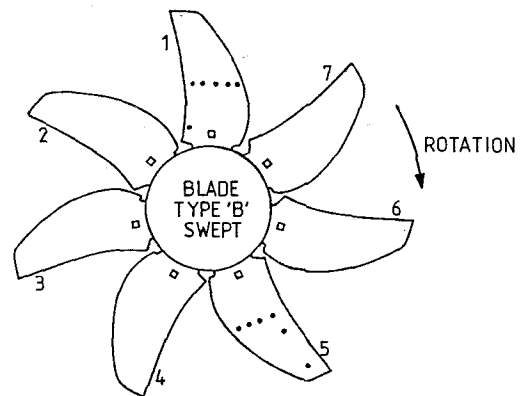
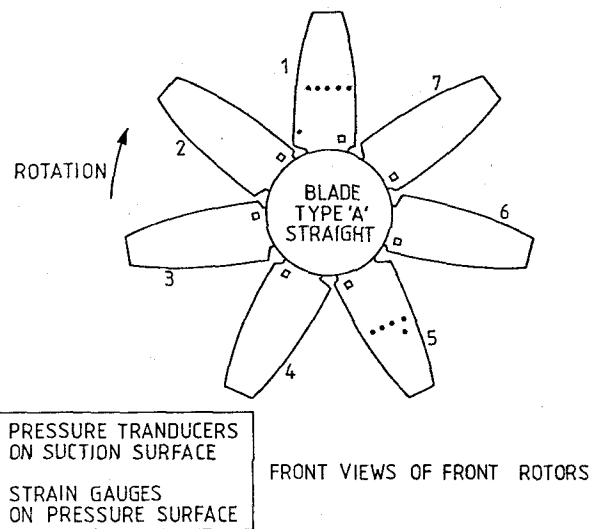


FIG 9 SCHEMATIC SHOWING LOCATIONS OF PRESSURE TRANSDUCERS AND STRAIN GAUGES ON BLADE TYPES A & B

- e) Provision of colour graphics displays of a menu-controlled set of selectable multi-parameter plots;
- f) Control of computer driven auto-traverse equipment for microphone noise field surveys;
- g) Network of audio links to provide communication between the test manager and function specialists together with a multi-location set of computer monitors displaying key test parameters.

As is evident from Fig 10, the task of overall test control was a complex one. At the planning stage, detailed attention was needed to all aspects of the task, particularly to interactions between systems and to coordination between system operators. A large team of specialists from Rolls-Royce, Dowty Aerospace and ARA carried out the tests and the success of the programme owes a great deal to their highly disciplined teamwork.

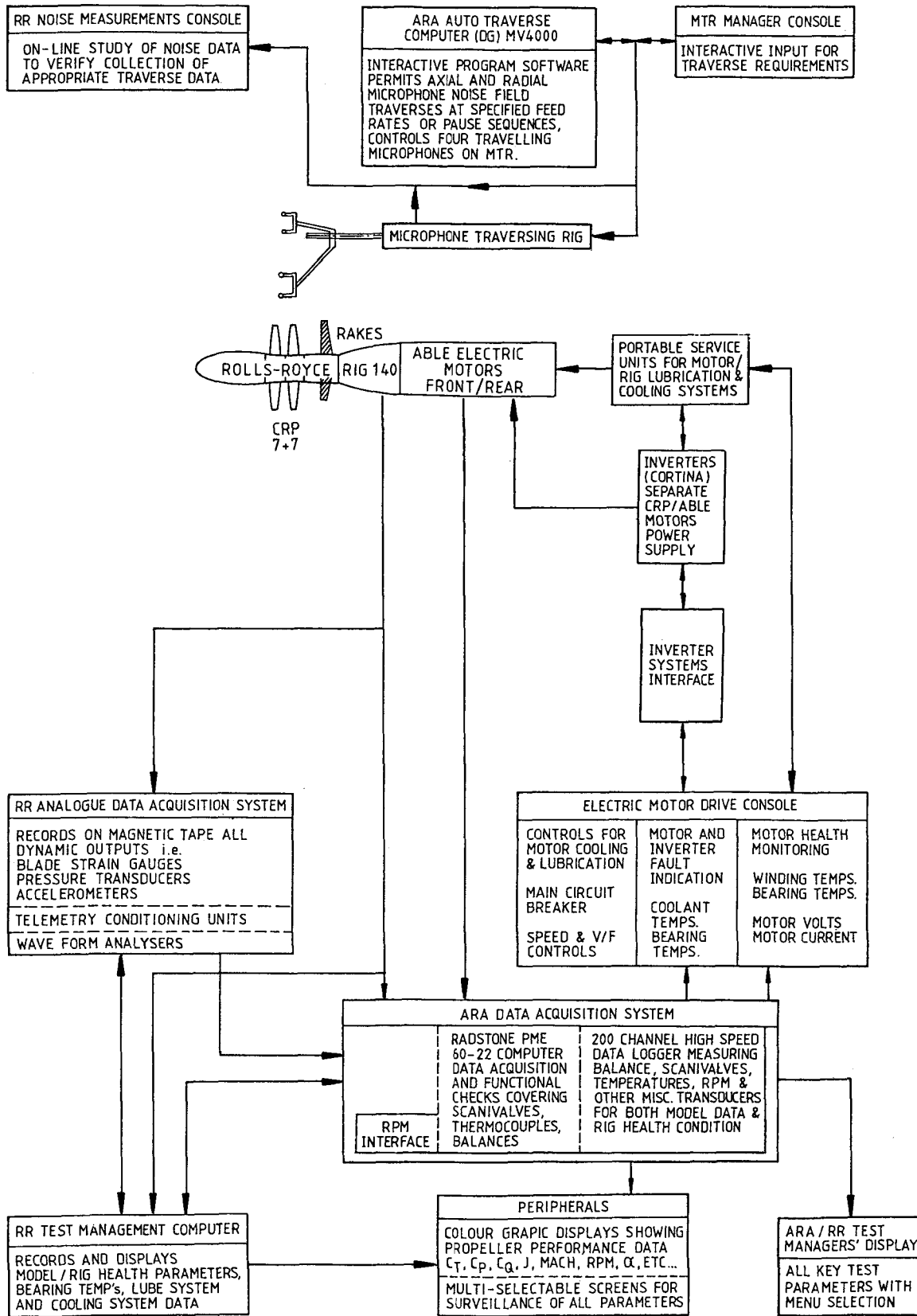


FIG 10 R12 PROPELLER RIG CONTROL, MONITORING & DATA ACQUISITION SYSTEM



#### 4.4 Laser Studies on Large Scale CRP Tests

Three separate laser techniques were used to provide research data during the large scale CRP test programme; all three techniques were created and directed by Rolls-Royce research team members.

##### Live Blade Twist Measurement Technique

The aerodynamic and centrifugal loads on the CRP blades cause the blades to deflect and twist, altering the pitch angle, aerodynamic loading and possibly sectional shape. To assess the magnitude of the twist and shape changes and thereby to assist with assessment and interpretation of measured to predicted performance variations, a laser system using an optical triangulation approach was used<sup>4</sup>.

The system measured blade shape for each of the blade rows (front and rear) at three selected radial stations. Previous experience of Rolls-Royce on turbofans had indicated that blade shape could be measured with an accuracy of a few thousandths of an inch. Interrogation of the data suggests that high accuracy was also obtained under the conditions imposed by the CRP transonic tunnel test requirements. The indications are that small variations in blade twist could be measured and that changes in blade camber could be observed.

##### Laser Anemometry

A key part of the Phase 2 tests in the basic TWT involved the use of a long throw two-spot laser transit anemometry (LTA) optical system. The LTA technique has the advantages that local velocity (speed and direction) can be measured by a non-intrusive approach and that quantitative information on turbulence level<sup>5</sup> can be obtained. Disadvantages are that the method requires significant elapsed time to collect the data and that an oil-mist flow-seeding system is required to provide particle paths.

Oil mist particles passing through the zone into which the laser beams are focussed create scattering of the light beam; these variations of light level are recorded using photomultipliers and a correlation of the derived signals permits evaluation of the velocity. The method uses two pairs of focussed beams, the orientation and position of the meeting points of which can be rotated and translated to enable velocities to be determined over a volume of the flow field.

A special laser cart, mounted in the tunnel floor, was used to carry the LTA equipment including the Argon Ion laser and a large mirror and related traversing equipment. The data processing and control of the laser was established in the TWT control room. Views of the laser cart and typical beam paths are shown in Figure 11. To relate the laser instantaneous measurements to rotor blade position, a precisely timed signal was created using a transverse pair of HeNe laser beams. The flow was seeded by plumes of 0.5  $\mu\text{m}$  particles of mineral oil injected from a special strut erected in the TWT settling chamber.

The LTA system was used to collect data for various locations in the CRP flow field including:

- Overtip vortex region
- In-rotor (between blades) region
- Between rotors region,
- Upstream and downstream of the rotors.

The capability to generate substantial sets of CRP velocity field data using the LTA system was demonstrated for both high and low speed test conditions.

##### Laser Holographic CRP Flow Visualisation

A non-intrusive double-pulse laser holographic flow visualisation system was used to produce interferometric holograms of the flow in the large scale CRP tests<sup>6,7</sup>. The beam from a high power pulsed laser (class IV) was used to illuminate the CRP model as shown in Figure 12. The method offered the advantage of being relatively rapid and it was practical to create 80 holograms in a single run of the order of one hour duration, including CRP power level changes and laser resetting.

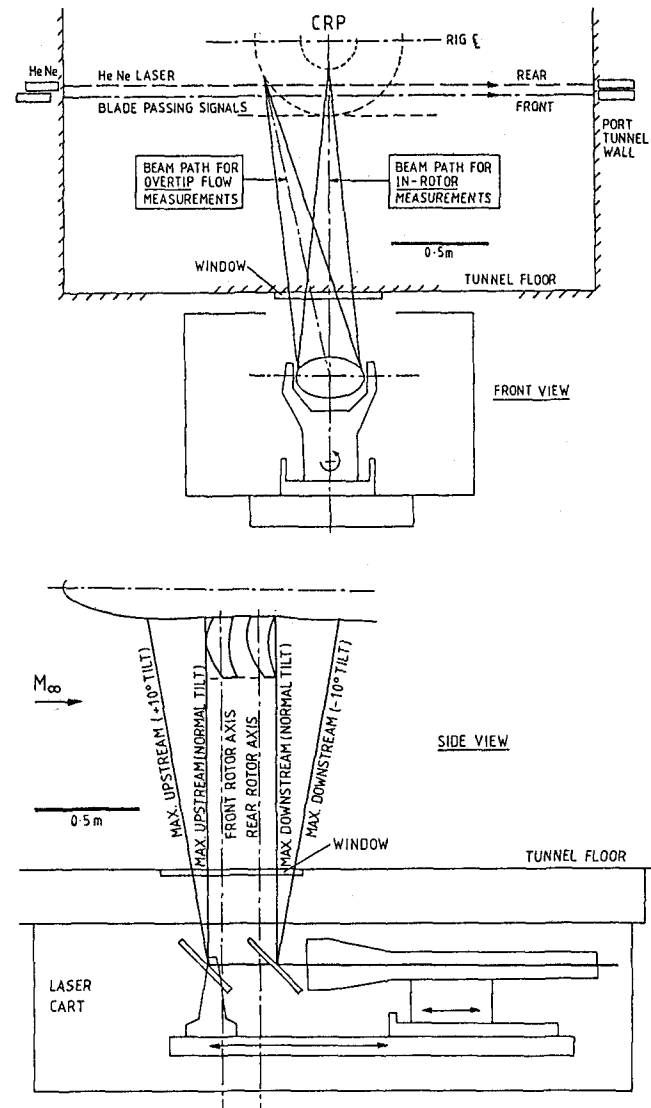


FIG 11 LASER CART WITH OPTICAL HEAD FOR LTA

Safety was keenly observed during all laser operations and an incident free series was achieved. Alignments of the optical system were performed using low power lasers.

The LTA and laser holographic systems were designed so as not to create mutual interference.

A large number of valuable holographic images of the CRP flow field were produced and a number of significant features have been observed including:

- a) Tip vortex path and chopping of front vortex by rear rotor;
- b) Shear layer in blade wake region;
- c) Supercritical flow features including expelled blade leading edge bow shock.

Interpretation of holograms was aided and enhanced by a closed circuit video system.

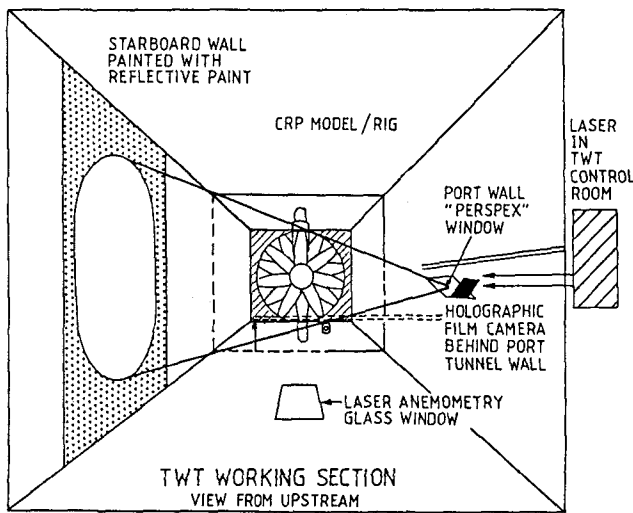


FIG 12 ARRANGEMENT OF LASER HOLOGRAPHIC SYSTEM IN TWT WORKING SECTION

#### 4.5 Development of the Acoustic Liner

##### General Requirements

An acoustic evaluation of the basic ARA tunnel was conducted in 1985 using a numerical model; this study indicated that the tunnel in its 'basic' form was unsuitable for acoustic measurements due to the strength of the reflections from the hard 22 ft (6.7 m) diameter pressure shell. This finding was confirmed by a brief set of measurements in the wind tunnel and was consistent with prior US experience<sup>8</sup> which had shown that lack of acoustic treatment could give rise to errors of the order of 5 dB in peak noise level.

Following this evaluation, a UK 'club' supported programme was launched to develop a removable acoustic liner for the tunnel. The development, reported more fully in Refs 9 & 10, required both aerodynamic and acoustic problems to be solved.

Aerodynamically, the acoustic liner was required to exhibit the following characteristics:

- a) Maximum practical working section cross sectional dimensions to maximise allowable model scale.
- b) Working M range from 0.2 to 0.85 with the main emphasis in the region 0.6 to 0.8.
- c) Uniformity of local Mach number to  $\pm 0.005$  in the region of the propeller.

Acoustic requirements were:

- a) Attenuation of incident sound waves over a wide bandwidth, especially in the propeller plane, to enable free field sound measurements to an accuracy of  $\pm 1$  dB or better;
- b) The ability to make noise measurements along axial, radial and circumferential lines.

The second requirement led to the development of a computer controlled microphone traversing rig system in parallel with the development of the acoustic liner.

##### Acoustic Design of the Liner

A numerical model was created by Rolls-Royce of a sound field in the wind tunnel. This model was used to represent various wall boundary conditions in combination with sound fields of prescribed directivity. The numerical model was based on decomposition of the sound field into plane wave rays; the direct and reflected field strengths were summed at a selected set of 'observer' locations. It was further refined using the concept that multiple reflections of the source sound field would arise and that the strength of the observed reflections would depend upon the positions of the source and observer within the tunnel and the reflection coefficients of the tunnel walls.

Subsequently, the model was extended to include the influence of freestream Mach number and the refraction of oblique incident waves by the tunnel wall boundary layers. Various source directivity patterns were considered including simplified models representative of SRP and CRP open rotors.

Using this numerical model, design studies were carried out to establish an acoustic treatment which would be an acceptable compromise between achieving good sound absorption and keeping the wall thickness of the liner to a practicable minimum. The requirement that the depth of an acoustic bulk absorber should be at least one quarter of a wave length for the lowest frequency of concern led to the selection of an absorber depth of 6 inches (0.15 m), corresponding to a wavelength of 2 feet (0.60 m) which would be obtained at a frequency of 570 Hz and a local speed of sound of 1140 ft/sec (347 m/s). To obtain a wide bandwidth of acoustic attenuation, an open cell polyurethane foam was chosen as the material for the bulk absorber.

The inner airswept surface of the liner was made of perforated steel sheet with an open area ratio close to 37%, which was predicted to be essentially transparent acoustically in the frequency range of interest. The chosen depth of absorber reduced the working section of the tunnel from 9' x 8' (2.7 m x 2.4 m) to 8' x 7' (2.4 m x 2.1 m) approximately.

### Aero/Mechanical Aspects of Liner Design

In aerodynamic terms, the design of the liner represented a significant challenge, given the aforementioned stream uniformity requirements. A joint computational/experimental approach was used to generate a suitable bellmouth inlet contraction design, to define longitudinal area variation, and to develop a diffuser arrangement compatible with the presence of the bulky model support strut. Ahead of the R12 programme, because of concerns regarding the high blockage of the rig in the liner, a set of TWT tests was made using a dummy rig in the tunnel with liner; these tests also included an investigation of the influence of the movement of the microphone traversing rig on longitudinal velocity distribution. The computational model (SPARV) used to design the liner was also used to support the analysis of measurements taken during these testing phases.

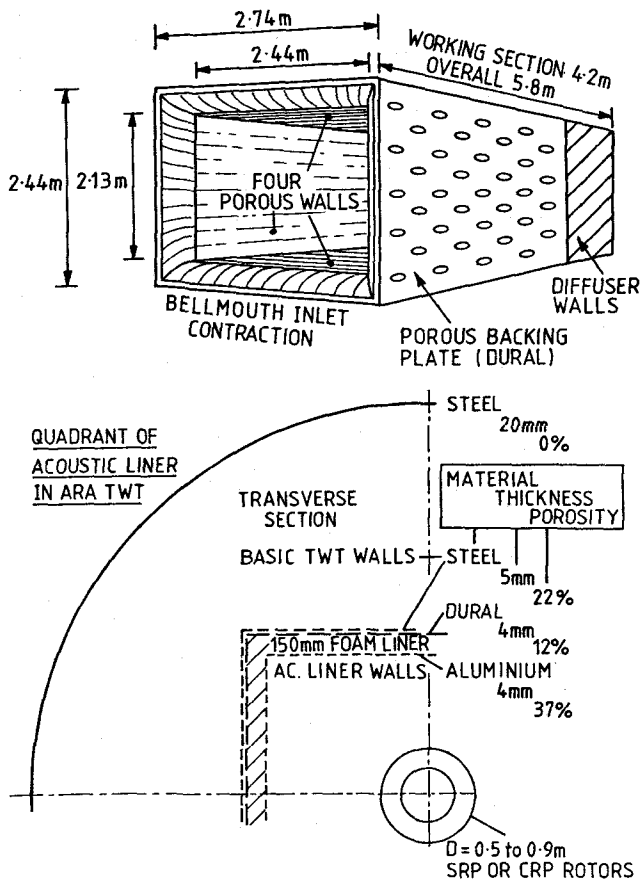


FIG 13 DETAILS OF ACOUSTIC LINER FOR ARA TRANSONIC TUNNEL

The mechanical design of the liner and its location with respect to the wall of the tunnel plenum chamber is illustrated in Fig 13. The liner has been built as a free-standing rectangular shell formed so as to retain the essential acoustic properties at the walls and to include an inlet bellmouth contraction and an outlet diffuser section. It fits closely within the existing TWT porous (22%) walls and provides a 12 ft (3.7 m) length of acoustically treated surface, which is considered sufficient to cover all likely model test requirements. A boundary layer bleed is provided to suppress separation at the corner

between the inlet contraction and the TWT walls. The foam is carried between longitudinal rails which serve as structural members and to which the inner walls (37% porosity) are fixed using discrete domed-head fixations to local hard points in order to minimise sound reflections. The rear wall of the liner is ventilated, for structural and aerodynamic rather than acoustic reasons.

The wind tunnel circuit has a removable section, immediately downstream of the test section, which is drawn back to enable model support carts to be interchanged. The same process provides access for inserting the acoustic liner into the tunnel, installation requiring slightly more, and removal rather less, than a working day.

### Acoustic Liner Proving Trials

Aerodynamic calibration of the liner in the TWT was carried out in three phases. In the first phase, tests with a long static probe on the axis of the empty liner established the flow uniformity in the liner and were used to develop procedures for tunnel setting and operation and for calculating Mach number in the liner. In the second, the effects of the microphone traverse rig and a small propeller rig were established and measurements of propeller performance were shown to match results in the standard (unlined) tunnel. The third phase, which involved tests with the dummy R12 rig, led to aerodynamic modifications to the liner diffuser which restored lost power margins and enabled the tunnel to be controlled up to a Mach number of 0.8 with the R12 model installed in the liner.

The calibration showed the freestream Mach number in the acoustic liner to be predominantly a function of the standard tunnel power setting parameters, fan speed etc, and secondarily dependent upon the level of plenum chamber suction; furthermore, the presence of the thrust producing CRP was expected to be significant. The liner Mach number calculation routine was based on the conventional approach to model blockage and included an allowance for tunnel wall constraint as well as model support interference and the effect of the presence of the microphone traverse rig. Tests have systematically included measurements of wall static pressures as well as upstream and plenum chamber pressures.

The acoustic development of the liner<sup>9,10</sup>, carried out under the R7 'club' programme, involved a series of tests with propellers in the lined TWT, backed up by acoustic trials with the liner outside the tunnel. Propeller tests in a low speed anechoic tunnel at RAE Farnborough provided a valuable datum.

The microphone traverse gear enabled longitudinal traverses to be made at a given radial distance from the axes but at different angles of azimuth (and therefore with different intensities of sound reflection from the walls). Traverses could also be made at the same azimuth but different radial distances.

The first trials of the acoustic liner showed unacceptable reflections from some features within the liner. The reflections were manifest as differences in field shape at different azimuth angles and as departures from the inverse square law along a ray path. By an iterative process,

which involved significant changes to the mechanical design of the liner, the sources of reflection were identified and eliminated. The final trials in the R7 programme, which were with a single rotation propeller of 15" diameter, showed that a high level of anechoicity had been achieved. At Mach numbers less than approximately 0.6, inverse square law behaviour was observed in the far field and directivity patterns measured at different azimuths matched each other closely. Above  $M = 0.6$ , reflections from the wall became increasingly obtrusive, particularly in the forward arc. Despite these reflections, attributable to boundary layer refraction, the liner was considered to provide adequate measurements of the key noise parameters at Mach numbers characteristic of propeller aircraft at cruise.

#### 4.6 Large Scale CRP Performance and Noise Measurements

As already stated, the tests of the large scale CRP in the ARA transonic wind tunnel were undertaken in two phases, viz:

Phase 1 (MAY/JUNE '89) CRP performance and noise measurements using Microphone Traversing Rig (MTR) and shaft balances in the TWI with acoustic liner fitted;

Phase 2 (OCTOBER '89) CRP flowfield surveys with performance measurements using laser transit anemometry and laser holographic techniques.

Prior to the first tunnel tests, however, an exhaustive check-out of the rig, its ancillary systems and its instrumentation was carried out in the test cell of the ARA Propeller Test House (PTH). The PTH was built as an adjunct to the overall propeller programme, to provide the capability, outside the tunnel, of exercising propeller rigs and their systems over as wide an operating range as possible at nominally static conditions. It has proved invaluable in the final, pre-tunnel stage of development and proving in all the rotor programmes.

#### Rotor Blade Stress, Vibration and Flutter Clearance

Although the proving trials in the PTH provided information on rig and rotor dynamics over the range of conditions achievable at nominally zero forward speed, the full dynamic clearance of the R12 rig had to await the first entry into the transonic tunnel. Thus, at the outset of the Phase 1 tests in the acoustically lined tunnel, it was necessary to 'clear' each of the rotors from the viewpoint of stress, vibration and flutter. Whilst critical rotational speeds are comparatively predictable from established rotor natural frequency (flap, torsion) data, the occurrence of classical flutter is far less predictable. The primary variable in classical flutter assessments is helical tip Mach number.

Tests to clear the rotors were performed by a carefully monitored sequence of rotor and tunnel speed variation as illustrated in, Fig 14. At a given tunnel Mach number, the speed of each rotor in turn was progressively increased until the limit of the test envelope was reached: rotor speed was

then reduced, tunnel Mach number increased without exceeding the safe helical tip Mach number established at the previous tunnel Mach number, and the process repeated. The flutter clearance tests were carried out for a single setting of the rotor blades and so provided a good first assessment rather than a full clearance of the rotor. Blade stress and vibration levels were therefore monitored carefully through the entire programme.

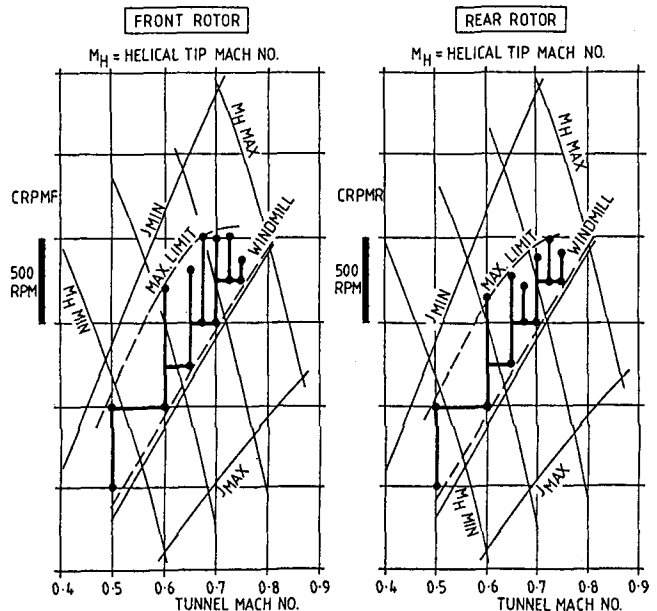


FIG 14 ON-LINE DISPLAY FOR STRESS AND VIBRATION SURVEY AT FIXED ROTOR BLADE ANGLES

#### Performance Testing

The specific objectives of the performance testing were as follows:

- Determine efficiency at key take-off, climb and cruise operating points;
- Examine a range of torque splits;
- Examine speed differentials at constant thrust and power;
- Determine efficiency and general performance over the Mach number range of 0.2 to 0.8.

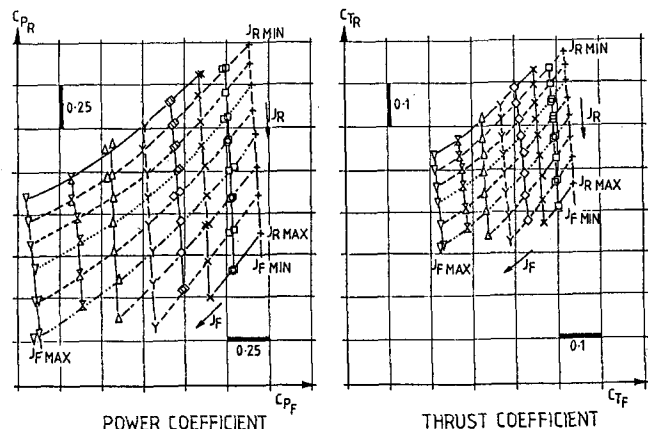


FIG 15 OPERATING MAP FOR LARGE SCALE CRP AT CRUISE DESIGN BLADE ANGLES & MACH NUMBER

The ease of speed control of the Able electric motors made it practical, in short time, to examine a matrix of front and rear power settings. Figure 15 shows the measured variations of thrust and power coefficient for the swept blades set at the established cruise blade angles. It is apparent that the performance of the CRP can be assessed over a fine mesh of the front and rear rotor advance ratios.

From tests covering a sweep of variables, as illustrated in Figure 15, specific levels of power and/or thrust coefficient were selected for further study using the noise survey equipment. This approach was very economical of tunnel time: typically, the performance points were collected at between one and two points per minute, while noise traverses usually took an order of magnitude longer.

As Fig 15 shows, the thrust and power coefficients exhibit typical CRP characteristics, namely that the front rotor directly influences rear rotor coefficients whilst the rear rotor has relatively little influence on front rotor coefficients. By basing the pattern of testing on this recognised characteristic, risks of exceeding rotor blade stress limits were reduced.

The measured CRP overall efficiency  $\eta$  (for combined front and rear rotors), derived from tests across a matrix of blade angle settings and front and rear advance ratios, for take-off free stream conditions, is plotted in Figure 16; the plot shows  $\eta$  variations with overall thrust loading. The envelope of data shows the optimum value of overall efficiency that can be achieved for a given overall thrust loading. The 'optimum overall efficiency' curve provides a useful basis for making comparisons for different rotor speeds, blade angles and rotor designs.

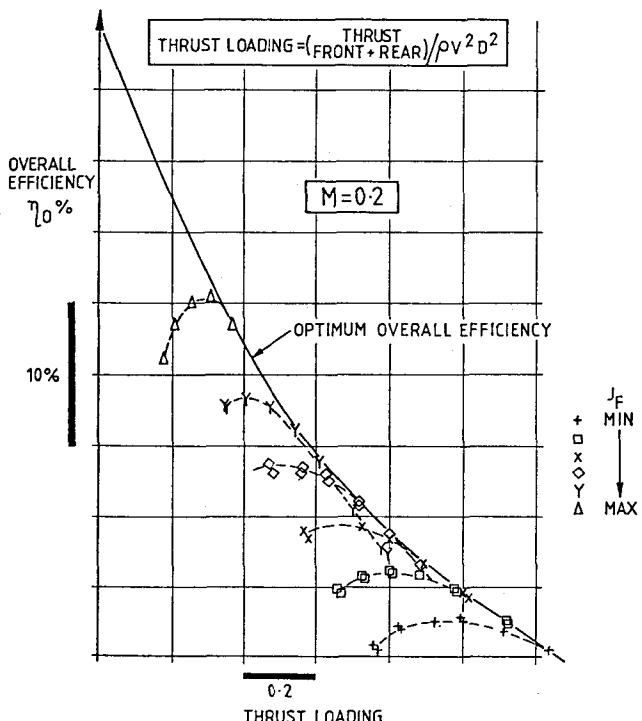


FIG 16 VARIATION OF OVERALL EFFICIENCY WITH THRUST LOADING. SWEEPED BLADES AT DESIGN TAKE-OFF ANGLES

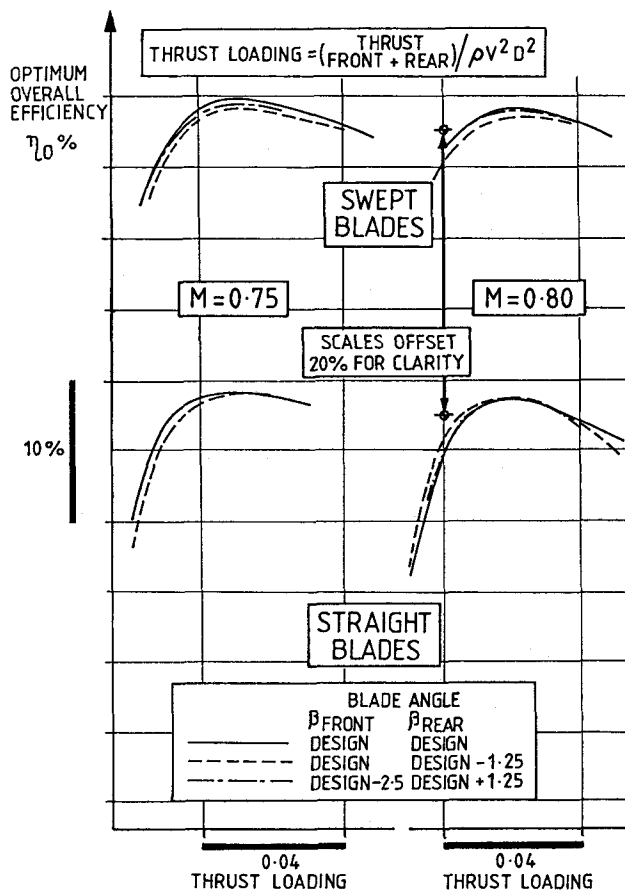


FIG 17 PERFORMANCE OF STRAIGHT AND SWEEPED BLADES AT HIGH SPEED CRUISE CONDITIONS

Comparative 'optimum overall efficiency' data for two of the rotor sets is shown in Figure 17 for a range of blade angle settings ( $\beta_F$ ,  $\beta_R$ ). It is clear that, at the higher cruise Mach numbers (0.75 to 0.8) the changes in blade angles have relatively minor effects on the optimum overall efficiency, whereas a significant variation with thrust loading is generally apparent. As expected, the swept blades achieved a higher efficiency at the cruise Mach levels than the straight bladed CRP when operated at realistically high thrust loadings.

An examination has been made of the reliability of the shaft balance data; this study was conducted in conjunction with the Phase 2 laser anemometry work.

The extended set of data samples at a nominally fixed set of test conditions (Mach number, advance ratios and blade angles) are shown in Figure 18 for thrust coefficient, power coefficient and efficiency; the data was collected during four separate tunnel runs of durations ranging from 20 to 150 minutes. The overall spread of the front and rear rotor data samples is of the order of one per cent for efficiency and 1 to 1½ per cent for thrust and power coefficients. On this basis, back-to-back testing should provide satisfactory discrimination of performance increments.

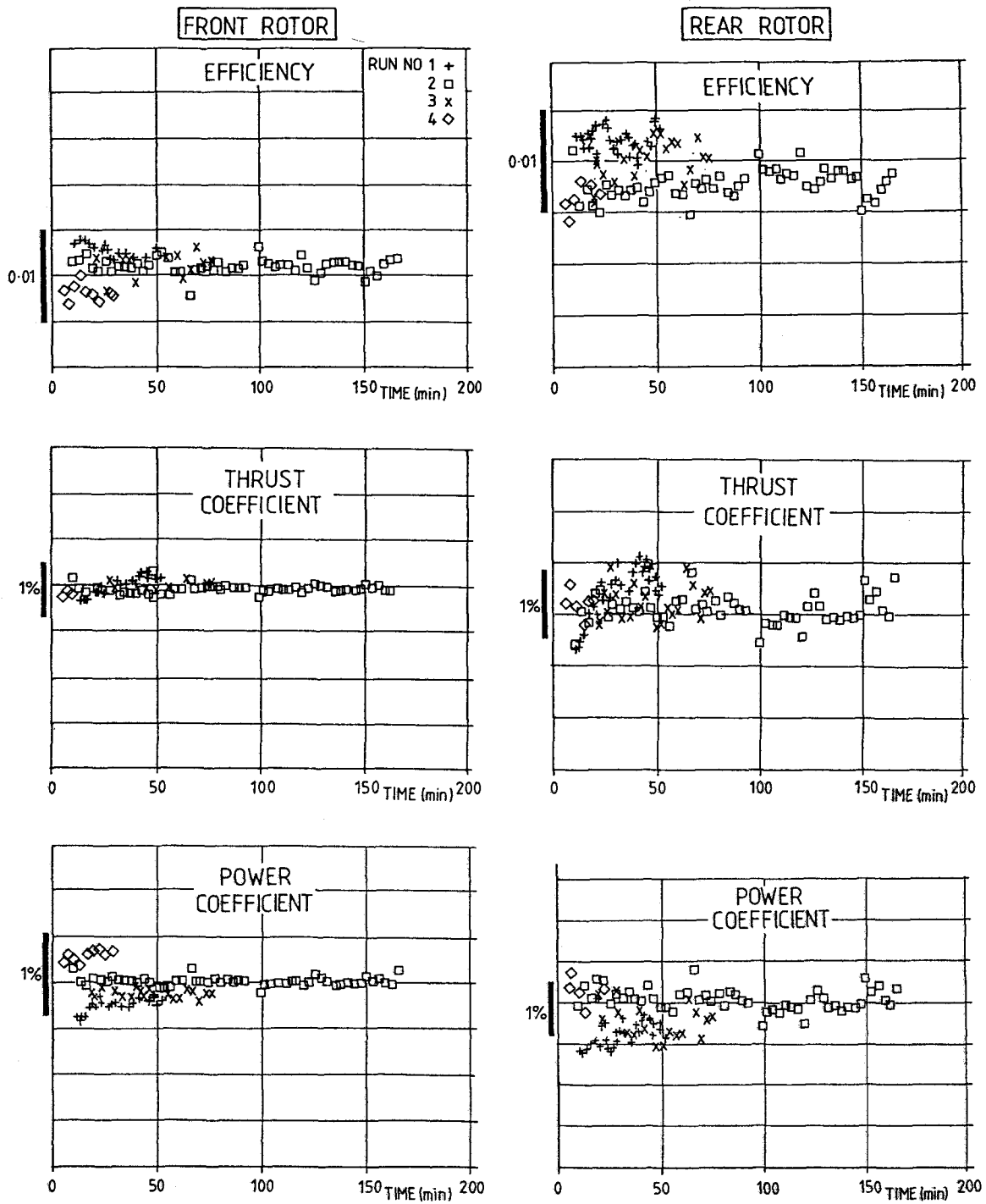


FIG 18 EXTENDED DATA SAMPLES AT FIXED OPERATING CONDITIONS SHOWING STABILITY OF SHAFT BALANCE MEASURED PERFORMANCE PARAMETERS

## Noise Measurements

In the course of the Phase 1 test entry, noise survey traverses were conducted for straight, swept (instrumented) and clean swept blade designs. The range of conditions covered freestream Mach numbers from 0.2 to 0.8 in combination with a wide range of rotor blade angle settings ( $\beta_F$ ,  $\beta_R$ ) and various power settings.

Fig 19 shows the microphone traverse rig and the positions of the traversing microphones, and also the fixed wall and blade mounted microphones, in relation to the rotor. In the configuration illustrated, the rig carried two pairs of microphones located at 19 inch and 30 inch sidelines (0.63 and 1.0 rotor diameters) which were traversed axially to provide noise field directivity, power and frequency spectra. A second configuration, with a single microphone which could be positioned anywhere within a circle of 54 inch diameter centred on the rig axis, was used for detailed measurement of radial and azimuthal variations of the sound field. In practice, it was shown that close pass traverses could be performed to within 0.05 rotor diameters of the blade tips.

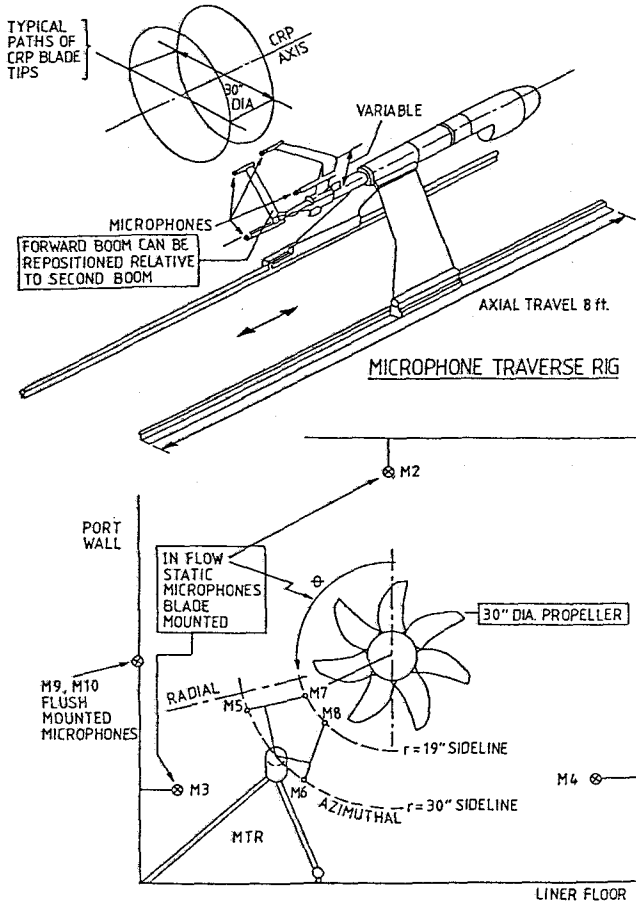


FIG 19 MICROPHONE LOCATIONS & MTR TRAVERSE PATHS

As noted in the previous section, noise measurements were made at selected points on the operating matrix of Fig 15. Some typical data are presented in Fig 20. Each graph gives the results for a pair of microphones at the same sideline distance but different azimuths, showing the field shapes given by the individual microphones and by their power-averaged mean. At a tunnel Mach number

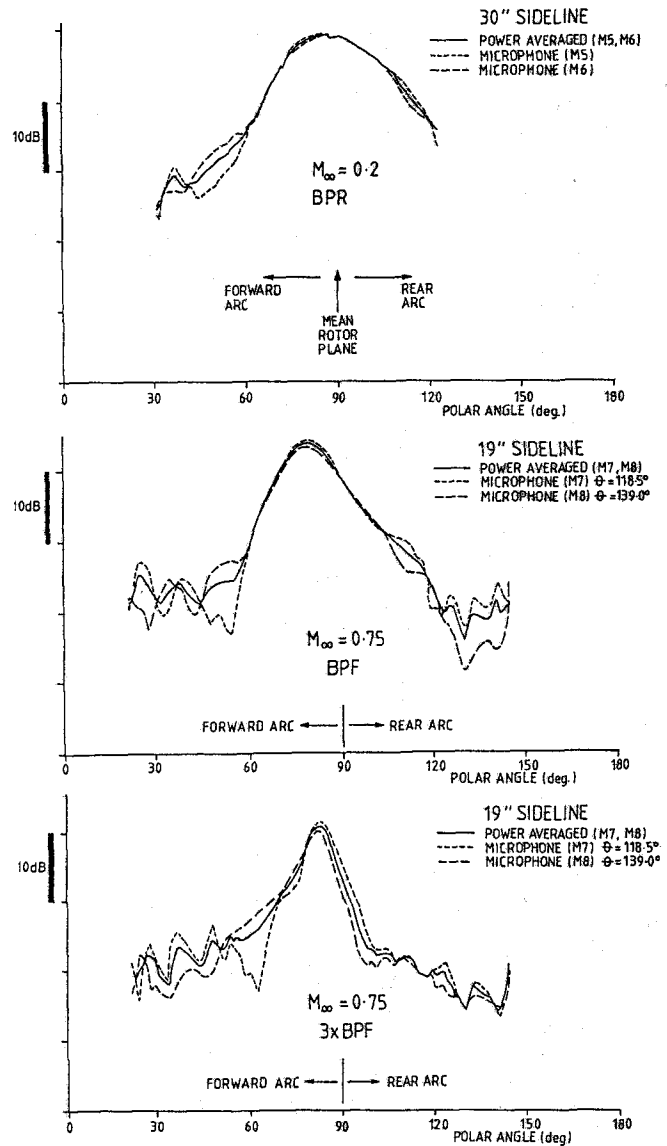


FIG 20 TYPICAL CRP NOISE DATA FOR LOW & HIGH TUNNEL SPEEDS & SELECTED FREQUENCIES

of 0.2 and at blade passing frequency, the results show very close agreement between the two microphones at the 30 inch sideline, indicative of the high degree of anechoicity achieved by the liner. At a tunnel Mach number of 0.75 at blade passing frequency, the microphones at the 19 inch sideline show close agreement in the region of peak noise but evidence of reflections in the forward and rearward arcs. At 3 times blade passing frequency these reflections appear slightly stronger but the agreement between the two microphones at the noise peak is still reasonably good.

The more detailed radial and azimuthal traverses confirmed this general picture and reinforced the conclusions reached<sup>10</sup> at the end of the small scale SRP trials in the acoustic liner. In particular, it was found over much of the Mach number range that the azimuthal variation in the sound field was small and that there was a significant region of the field in which the inverse-square decay law was satisfied.

## 6 CONCLUDING REMARKS

- 6.1 A significant set of advances in wind tunnel technique for the study of high speed contra-rotating propellers has been achieved at ARA Bedford.
- 6.2 The techniques for small scale isolated and installed CRP rotor systems which have been developed will make a worthwhile contribution to the overall study of propeller installation technology.
- 6.3 Methods for the study of CRP designs at large model scale have been developed including performance measurement, noise field measurement, and flow field measurement and visualisation techniques.
- 6.4 Acoustic measurements with the large scale CRP have confirmed the earlier conclusion, from tests with a small scale SRP, that the acoustic liner is effectively anechoic.

## ACKNOWLEDGEMENTS

The extensive and invaluable support of all UK open rotor club members, BAe, RR and DA, as well as the DTI and our colleagues at ARA Ltd, is gratefully acknowledged herewith.

Specific mention must be made of the liaison of RR, DA and ARA in respect of the large scale studies reported herein which were also supported by RAE specialists and MOD contract AE/12a/89. The small scale studies included contributions from BAe and DA specialists as well as the use of the BAe owned TD1700 air motor.

## REFERENCES

- 1 Beavis D G, Pozniak O M, 'Facilities for the development of propellers and propeller installations at ARA', RAeS Conference Advanced Propellers and their Installation on Aircraft, Paper 8, Sept 1988.
- 2 Harris A E, Paliwal K C, 'Civil turbofan propulsion system integration studies using powered testing techniques at ARA Bedford', AIAA 84-0593, 1984.
- 3 ESDU, 'Thrust and drag accounting for propeller/airframe interaction', Item No 85017, Nov 1985.
- 4 Davinson I et al, 'Optical fan blade profile measurements in rotating turbofans', ASME 90 Turbo Expo, to be published.
- 5 Haxell C F, 'Laser anemometry in rotating transonic flows', 6th International Conference on Photon Correlation and Other Optical Techniques in Fluid Mechanics, Cambridge, July 1985.
- 6 Parker R J, Jones D J, 'The use of holographic interferometry for turbo machinery and evaluation during rotating tests', Journal of Turbomachinery, Vol 110, pp 393-400, 1988.
- 7 Parker R J, Jones D J, 'Holographic flow visualisation in rotating transonic flows', Institute of Physics Conference Series No 77, pp 141-146, 1988.
- 8 Glover B M, Plunkett E I, Simcox C D, 'Noise testing of an advanced propeller in the Boeing transonic wind tunnel with and without test section acoustic treatment', AIAA Paper no 84-2366.
- 9 Wood M E, Newman D A, 'The design and development of an acoustic test section for the ARA transonic wind tunnel', Royal Aeronautical Society paper, Sept 1988.
- 10 Wood M E, Newman D A, 'The design and commissioning of an acoustic liner for propeller noise testing in the ARA transonic wind tunnel', SAE Aerotech '89, C398/25, Engine and Instrumentation, 1989.